



Published in final edited form as:

*Int J Cancer*. 2010 January 15; 126(2): 533–544. doi:10.1002/ijc.24725.

## Inhibition of ovarian cancer cell proliferation by a cell cycle inhibitory peptide fused to a thermally responsive polypeptide carrier

Iqbal Massodi, Shama Moktan, Aruna Rawat, Gene L. Bidwell III, and Drazen Raucher\*  
Department of Biochemistry, University of Mississippi Medical Center, Jackson, MS 39216

### Abstract

Current treatment of solid tumors is limited by normal tissue tolerance, resulting in a narrow therapeutic index. To increase drug specificity and efficacy and to reduce toxicity in normal tissues, we have developed a polypeptide carrier for a cell cycle inhibitory peptide, which has the potential to be thermally targeted to the tumor site. The design of this polypeptide is based on elastin-like polypeptide (ELP). The coding sequence of ELP was modified by the addition of the cell penetrating peptide Bac-7 at the N-terminus and a 23 amino acid peptide derived from p21 at the C-terminus (Bac-ELP1-p21). Bac-ELP1-p21 is soluble in aqueous solutions below physiological temperature (37°C) but aggregates when the temperature is raised above 39°C, making it a promising thermally responsive therapeutic carrier that may be actively targeted to solid tumors by application of focused hyperthermia. While Bac-ELP1-p21 at 37°C did not have any effect on SKOV-3 cell proliferation, the use of hyperthermia increased the antiproliferative effect of Bac-ELP1-p21 compared with a thermally unresponsive control polypeptide. Bac-ELP1-p21 displayed both a cytoplasmic and nuclear distribution in the SKOV-3 cells, with nuclear-localized polypeptide enriched in the heated cells, as revealed by confocal microscopy. Using Western blotting, we show that Bac-ELP1-p21 caused a decrease in Rb phosphorylation levels in cells treated at 42°C. The polypeptide also induced caspase activation, PARP cleavage, and cell cycle arrest in S-phase and G2/M-phase. These studies indicate that ELP is a promising macromolecular carrier for the delivery of cell cycle inhibitory peptides to solid tumors.

### Keywords

Elastin-like polypeptide; p21; Hyperthermia; Thermal targeting; Drug delivery

### Introduction

Current cancer therapy is limited by the extreme toxicity of chemotherapeutic drugs, which can cause extensive damage to non-cancerous tissues when administered in doses required to eradicate cancer cells. Therefore, it is necessary to develop new targeted therapeutic approaches to make chemotherapeutics more site specific and less toxic to normal tissues. Numerous drug delivery systems have been previously devised for targeted drug delivery including liposomes,<sup>1</sup> 2 microspheres and nanospheres,<sup>3</sup> macromolecular synthetic polymers,<sup>4–8</sup> etc. Many macromolecular carriers are already employed in the advanced stages of drug development due to the fact that they impart enhanced stability and

\*Correspondence to: Department of Biochemistry, University of Mississippi Medical Center, 2500 North State Street, Jackson, MS 39216, Phone: 601-984-1510, Fax: 601-984-1501.

Novelty and impact: This study describes a novel thermally responsive macromolecular carrier for the targeted delivery of a cell cycle inhibitory peptide to solid tumors. The study can have an impact on the targeted therapy of solid tumors.

therapeutic efficacy to low molecular weight drugs. Another advantage of using macromolecules in the treatment of solid tumors is that polymer-drug conjugates preferentially accumulate in tumors as a result of the enhanced permeability and retention effect (EPR).<sup>9–12</sup> EPR is a phenomenon in which macromolecular drugs are retained in the tumor due to their leaky vasculature and poor lymphatic drainage. In addition to the EPR mediated passive targeting by macromolecular carriers, active targeting can also be achieved by delivering the chemotherapeutic drug specifically to the tumor site. In addition to passive and active accumulation of the drug at the tumor site, chemotherapy can also be improved by developing therapeutic agents which are exclusively toxic to the cancer cells. The work described here combines all of these approaches to develop a peptide inhibitor that can be actively targeted to the tumor site and is capable of arresting the cell cycle.

One approach in therapeutic drug design is to target cellular pathways that are often deregulated in cancer cells. Inhibition of the cell cycle is one of the attractive targets for cancer therapy. Numerous cell cycle inhibitors have been well characterized previously, and p21 and p16 mimetic peptides showing a great potential as chemotherapeutic agents.<sup>13–16</sup> However, peptide based drugs have limited cellular access and poor pharmacokinetic parameters, rendering them ineffective *in vivo*. By conjugating peptides to cell penetrating peptides and macromolecular carriers, cell permeability and pharmacokinetic characteristics of therapeutic peptides may be dramatically improved.

In this study, we present a targeted drug delivery approach using the thermally responsive macromolecular carrier elastin-like polypeptide (ELP) for intracellular delivery of a therapeutic peptide. ELP is a biopolymer derived from the structural motif found in mammalian elastin protein, which consists of pentapeptide Val-Pro-Gly-Xaa-Gly (VPGXG) repeated 150 times, where Xaa, a “guest residue”, is any amino acid except Pro.<sup>17–18</sup> ELPs are soluble in aqueous solution below their transition temperature ( $T_t$ ). However, when the temperature is raised above their  $T_t$ , they undergo a reversible phase transition, forming aggregates which appear as an insoluble cloudy solution. This cloudy solution turns clear again on lowering the temperature below  $T_t$ . Based on this property, ELP has the potential to be used as a thermally targeted drug delivery vector. Our hypothesis is that intravenously delivered anticancer therapeutics conjugated to ELP will accumulate at the tumor site where local hyperthermia is applied ( $T > T_t$ ). However, they will be cleared under normal physiological conditions and temperature ( $T < T_t$ ), where these ELP carriers will be in their soluble state. This hypothesis is supported by a previous *in-vivo* study of ELP delivered to human tumors implanted in nude mice. A 2-fold increase in ELP accumulation was observed in heated tumors as compared to non-heated tumors, on systemic administration of ELP.<sup>19–20</sup> The accumulation of ELP in the extravascular compartment was further enhanced by employing “thermal cycling”.<sup>21</sup> Hyperthermia itself enhances the permeability and perfusion of tumor vasculature as compared to normal vasculature and may therefore further enhance the drug delivery.<sup>22–24</sup> Therefore, the use of ELP as a therapeutic vector combines the advantages of passive targeting due to its macromolecular nature and active targeting due to the accumulation of thermally responsive ELP upon application of hyperthermia.

One of the problems in efficient delivery of drugs by macromolecular carriers is their inability to efficiently translocate across the cell membrane because of its lipophilic nature. One way to overcome this problem is to conjugate these macromolecules to cell penetrating peptides (CPPs). CPPs are short, 10–30 amino acid peptides that are able to efficiently translocate various cargo into the cells.<sup>25–28</sup> In our previous study, we have shown that different CPPs (Antp, Tat, and MTS) were able to translocate ELP across the cell membrane.<sup>29</sup> In addition, Antp was used to deliver a p21 mimetic peptide capable of inhibiting the proliferation of HeLa and SKOV-3 cells. We have also shown that the fusion

of the Tat peptide dramatically increases the internalization of thermally responsive ELP1 and ELP1-GFLG-Dox upon application of hyperthermia.<sup>30, 31</sup> More recently, we have modified the coding sequence of the thermally responsive ELP at the N-terminus by addition of a transduction domain from Bac-7.<sup>32</sup> Bac-7 belongs to the bactenecin family of antimicrobial peptides, and we have shown that fusion of the Bac CPP to ELP causes a portion of the polypeptide in the cell to reach the nucleus.<sup>33</sup> The current study expands the previous work by using the Bac CPP to deliver ELP modified at its C-terminus with a p21<sup>WAF1/CIP1</sup> derived peptide (p21).<sup>34</sup> This p21 derived peptide has been shown to mimic the C-terminus of p21, interfere with PCNA function, and inhibit cyclin-CDK activity.<sup>15, 34, 35</sup> By conjugating the peptide to Bac-ELP, we show here that the polypeptide can be localized to the nucleus of SKOV-3 cells, where it arrests the cell cycle, induces caspase activation, and inhibits Rb phosphorylation. Furthermore and most excitingly, the proliferation inhibitory effects of this polypeptide were enhanced when hyperthermia was used to induce polypeptide aggregation and increase its cellular uptake. These results suggest that ELP-based therapeutics have great potential as targeted drug delivery systems for cell cycle inhibitory peptides such as p21.

## Material and methods

### Design of constructs

pUC19-ELP1 and pUC19-ELP2 were synthesized as described previously.<sup>30, 36, 37</sup> The ELP coding sequence was modified by the addition of the Bac (MRRIRPRPPRLPRPRRPLPFPPRP) coding sequence to the N-terminus and the p21 (GRKRRQTSMTDFYHSKRRLIFSKRKP) coding sequence to the C-terminus. Sequences of all synthesized constructs were confirmed by DNA sequencing.

### Polypeptide purification

pET25b+ expression vectors containing the desired constructs were transformed into *E. coli* BLR (DE3) (Novagen, Madison, WI) for protein hyperexpression.<sup>38</sup> Cells were then harvested by centrifugation and the protein was extracted as described previously.<sup>29, 37</sup>

### Characterization of transition temperature

The temperature-induced aggregation of the proteins was characterized by monitoring absorbance at 350 nm as a function of temperature. Solutions of Bac-ELP1-p21 and Bac-ELP2-p21, or their rhodamine labeled counterparts, containing 20  $\mu\text{mol/L}$  protein in PBS were heated or cooled at a constant rate of 1°C/min in a temperature-controlled multicell holder in a UV-visible spectrophotometer (Cary 100, Varian instruments). The  $T_t$  was defined as the temperature at which the  $A_{350}$  reached 50% of the maximum turbidity. In order to determine the effect of polypeptide concentration on the  $T_t$  under experimental conditions, a solution of 5, 10, 20, or 30  $\mu\text{M}$  Bac-ELP1-p21 in cell culture media was analyzed as described above. In order to determine the therapeutic concentration window (the concentrations at which the  $T_t$  is between 37 and 42 °C), the  $T_t$  was plotted versus polypeptide concentration, and this data was fit with a logarithmic equation.

### Conjugation of polypeptides with fluorescent probes

In a conjugation reaction, proteins were diluted to 100–200  $\mu\text{M}$  in PBS, and tris-(2-carboxyethyl) phosphine (TCEP) was added to a 10-fold molar excess. A thiol reactive probe (tetramethylrhodamine-5-iodoacetamide dihydroiodide; Molecular probes, Eugene, OR) was slowly added, while mixing to a final two-fold molar excess, and then incubated with continuous stirring for 2 h at room temperature or overnight at 4°C. The reaction was then quenched by adding an excess of  $\beta$ -mercaptoethanol, and the unreacted label was

removed by extensive dialysis in PBS followed by two to three thermal cycles. Efficiency of the labeling on the single cysteine residue was assessed by UV-visible spectrophotometry (UV-1600 Shimadzu). The molar label to protein ratio was 0.3–0.5.

### Cell culture and polypeptide treatment

Ovarian cancer cells SKOV-3 (ATCC, Manassas, VA) cells were grown in McCoy's-5a media (Invitrogen) supplemented with 10% fetal bovine serum (Sigma), 100 units/ml penicillin, 100 µg/ml streptomycin, and 25 µg/ml amphotericin B (Invitrogen, Carlsbad, CA). MCF-7 cells were grown in Minimal Essential Medium supplemented with 10% fetal bovine serum, 1 mM Sodium pyruvate, BME amino acids, 5 µg/ml insulin (Sigma), 100 units/ml penicillin, 100 µg/ml streptomycin, and 25 µg/ml amphotericin B (Invitrogen). Panc-1 cells were grown in Dulbecco's Minimal Essential Medium (Invitrogen) supplemented with 10% fetal bovine serum (Sigma), 100 units/ml penicillin, 100 µg/ml streptomycin, and 25 µg/ml amphotericin B (Invitrogen). Cultures were maintained at 37°C in a humidified atmosphere + 5% CO<sub>2</sub>. For experiments, cells were removed from tissue culture flasks by brief treatment with 0.05% v/v trypsin-EDTA (Invitrogen) and plated in 6 well plates (500,000 cells/ well) for flow cytometry, in 96 well plates (6000 cells/ well) for proliferation, and in 24 well plates (12,000 cells/well) for proliferation rate. Twenty-four hours after plating, cells were treated with media containing the indicated concentration of polypeptides for 1 h, rinsed, and replaced with fresh media.

### Cell proliferation

SKOV-3 cells were plated at 6000/ well in 96 well plates and treated with Bac-ELP1-p21, Bac-ELP2-p21, Bac-ELP1, ELP1-p21 and p21 peptide at various concentrations for 1 h at 37 °C or 42°C. Cells were washed, and fresh media was replaced. Cell proliferation was measured at the indicated time using the MTS assay. The effect of polypeptides on the proliferation rate of SKOV-3 cells was determined by plating 12,000 cells/ well in a 24 well plate. Cells were treated with Bac-ELP1-p21 or Bac-ELP1 (20 µM) for 1 h at 37 or 42°C, and the cell counts were made daily using a Coulter counter (Coulter, Fullerton, CA).

### Laser scanning confocal fluorescence microscopy

SKOV-3 cells were plated in 6 well plates on coverslips and allowed to grow overnight to 50% confluence. Cells were then treated with 20 µM rhodamine-conjugated Bac-ELP1-p21 for 1 h at 37 or 42°C, rinsed with PBS at the indicated times, fixed with PBS + 4% paraformaldehyde, and permeabilized with PBS + 0.025% Triton X-100. Cells were blocked with PBS + 1% BSA for 30 min at room temperature, stained with a monoclonal, FITC-conjugated  $\alpha$ -tubulin antibody (1:50 dilution, Sigma) and visualized using a TCS SP2 laser scanning confocal microscope with a 100× oil immersion objective (Leica, Wetzlar, Germany).

### Cell cycle analysis

SKOV-3 cells were plated in 6 well plates (500,000 cells/ well). Cells were then treated with 20 µM Bac-ELP1 or Bac-ELP1-p21 for 1 h at 37 or 42°C. After 1 h incubation, fresh media was added and cells were incubated at 37°C. After the indicated time intervals, the cells were washed with PBS and detached with trypsin. To this cell suspension RNase A (Sigma) was added to a final concentration of 750 µg/ml for 5 min., followed by 75 µg/ml propidium iodide (PI, Sigma) for 30 minutes at room temperature. The propidium iodide fluorescence was measured in channel FL3 using a Cytomics FC 500 flow cytometer (Becton Dickinson, San Jose, CA). A scatter plot of forward scatter vs. FL3 intensity was used to exclude cell debris and cell aggregates from the analysis. Histograms of PI intensity were gated into regions representing cell cycle phases to determine the percentage of cells in each phase of

the cell cycle using CXP software from Beckman Coulter. The data represents the average of at least 3 experiments; error bars, SEM.

To confirm the results of the PI staining, a BrdU (5-bromo-2'-deoxyuridine) incorporation assay was combined with PI staining. Cells were plated and treated as described above. 24 h after treatment, cells were exposed to 10  $\mu$ M BrdU for 1 h. Cells were rinsed, harvested by trypsinization, and fixed for 30 min on ice in 75% ethanol. Cells were suspended in 1 ml of 2 N HCl / 0.5% Triton X-100 for 30 min at room temperature to denature the DNA. Cells were spun and resuspended in 1 ml of 0.1 M Na<sub>2</sub>B<sub>4</sub>O<sub>7</sub>, pH 8.5, to neutralize the sample, then rinsed one time with PBS. After suspension in 75  $\mu$ L PBS + 0.5% Tween 20 / 1% BSA, RNase A (Sigma) was added to a final concentration of 750  $\mu$ g/ml, and mouse-anti-BrdU-Alexa 488 (Molecular Probes, Eugene, OR) was added to a final concentration of 100  $\mu$ g/ml. The sample was incubated overnight at 4 °C with gentle agitation. Cells were rinsed once with PBS and stained with 75  $\mu$ g/ml propidium iodide (Sigma) for 30 minutes at room temperature. Alexa 488 fluorescence was measured in channel FL1 and propidium fluorescence was measured in channel FL3 using a Cytomics FC 500 flow cytometer (Beckman Coulter, Fullerton, CA). A scatter plot of forward scatter vs. FL3 intensity was used to exclude cell debris and cell aggregates from the analysis.

### Caspase detection assay

SKOV-3 cells were plated at 500,000 cells/ well in a 6 well plate and treated with 20  $\mu$ M Bac-ELP1 or Bac-ELP1-p21 at 37°C or 42°C for 1 h. Fresh media was added to cells after the 1 h incubation. After the indicated time intervals, floating cells were collected, and attached cells were washed with PBS and detached using trypsin. Caspase activity was detected by staining both floating and attached cells with 10  $\mu$ l of 30 $\times$  carboxyfluorescein FLICA reagent for 2 h as per the protocol of FLICA-Apoptosis Poly-caspase Detection Kit (Immunochemistry Tech. Bloomington, MN). Cells were rinsed twice with apoptosis wash buffer and analyzed for caspase activation by flow cytometry using a Cytomics FC 500 flow cytometer (n = 5,000 cells). Forward versus side scatter gating was used to eliminate cell debris from the analysis, and the histogram of fluorescein fluorescence (channel FL1) was bimodal with peaks for caspase positive and caspase negative cells. The percentage of caspase positive cells was determined from the histograms and expressed as an average of at least 3 experiments; error bars, SEM.

For detection of PARP cleavage, cells were grown to 75% confluence in 75 cm<sup>2</sup> tissue culture flasks and treated with saline control, Bac-ELP1 (20  $\mu$ M), or Bac-ELP1-p21 (20  $\mu$ M) for 1 h at 37 or 42 °C. 24 h after treatment, floating and attached cells were removed from the flask, rinsed, and counted. Cells were resuspended in PARP gel loading buffer (65 mM Tris, 6 M urea, 26% glycerol (v/v), 2.1 % SDS (w/v), 0.01% bromophenol blue (w/v)) to a cell concentration of 1.5  $\times$  10<sup>6</sup> cells/mL and sonicated (2  $\times$  20 s cycles at 20 % amplitude using a Fisher Sonic Dismembrator and a microtip). The lysate was heated at 65 °C for 20 min and run on a 12 % polyacrylamide gel for 45 min at 200 V. The resolved gel was transferred to a nitrocellulose membrane by electroblotting in transfer buffer (25 mM Tris, 192 mM glycine, 20% methanol, 1% SDS) for 2 h at 40 V. The membrane was blocked with 3 % nonfat milk in PBS for 1 h and probed with PARP polyclonal antibody (Biomol, 1:250 dilution) overnight at 4 °C. The blot was rinsed and detected using a goat anti-rabbit horseradish peroxidase (HRP) conjugated secondary antibody (Pierce, Rockford, IL, 1:15,000 dilution) and Supersignal® West Pico chemiluminescent substrate (Pierce).

### SDS-PAGE and western blot analysis

SKOV-3 cells were plated at 1 $\times$ 10<sup>6</sup> in a 75 cm<sup>2</sup> tissue culture flask, grown overnight and treated with 30  $\mu$ M Bac-ELP1 or Bac-ELP1-p21 at 42°C for 1 h. Attached cells were

washed with PBS and harvested using trypsin 24 h after treatment. The cells were lysed by flash freezing the pellet in liquid nitrogen, followed by grinding with a pestle in 200  $\mu$ l lysis buffer (PBS + 0.25% Triton X-100). This lysed cell solution was further rotated for 1 h at 4°C. The cell lysate was cleared by centrifugation (13,000  $\times$  g for 2 min) and the total protein concentration was determined by a Bradford Assay. Equal amounts of total protein from each lysate were loaded on a 12% polyacrylamide gel. Electrophoresis and transfer were carried out as described above. The membrane was blocked with 3 % nonfat milk in PBS for 1 h and probed with rabbit polyclonal antibodies against the Rb or pRb proteins (Molecular Probes, 1:250 dilution) overnight at 4°C. The blot was rinsed and detected using a goat anti-rabbit horseradish peroxidase (HRP) conjugated secondary antibody and Supersignal® West Pico chemiluminescent substrate as described above. Equal loading was insured by reprobing the blot with mouse anti  $\beta$ -tubulin (Chemicon International, Temecula, CA, 1:10,000 dilution).

## Results

### Design and thermal properties of polypeptide

The drug carriers used in this study are based on elastin-like polypeptide (ELP), a macromolecular biopolymer composed of the pentapeptide repeat VPGXG, where “X” is a guest amino acid. ELPs are thermally responsive polypeptides that undergo an inverse temperature phase transition when the temperature is raised above its characteristic  $T_t$ . Two variants of ELP were used in this study, ELP1 and ELP2. ELP1 consists of 150 pentapeptide repeats with the guest position comprised of the amino acids V, G, and A in a 5:3:2 ratio. The group of polypeptides based on the ELP1 sequence has a  $T_t \sim 39\text{--}41^\circ\text{C}$ . ELP2 polypeptides contain 160 VPGXG repeats, where X is represented by V, G, and A in a 1:7:8 ratio. ELP2-containing polypeptides are used as controls for the effect of hyperthermia alone since they have a  $T_t \sim 65^\circ\text{C}$  and therefore do not undergo a temperature transition at the hyperthermia temperature

To facilitate the entry of the ELP polypeptide across the cell membrane, ELP was fused to the cell penetrating peptide Bac, a 24 amino acid peptide of the batenecin family. Bac has been shown to deliver cargo inside cells 32, 39, and we have used Bac to delivery ELP to the nucleus 33. The coding sequence of ELP was further modified with an inhibitory peptide derived from p21<sup>waf1/CIP</sup>, which is the C-terminal part of the full length p21 protein spanning amino acids 139–164.34 This C-terminal p21 fragment has been shown to exhibit cyclin-CDK inhibitory activity and also inhibit human cancer cell proliferation.16, 34, 40

Since these modifications of the ELP sequence often result in a change in the ELP  $T_t$ , we measured the  $T_t$  of Bac-ELP1-p21 and Bac-ELP2-p21. As the temperature of the ELP solution is increased above its  $T_t$ , there is a structural rearrangement of the protein which results in the formation of aggregates. When the temperature is lowered below the  $T_t$ , these aggregates re-solubilize. Formation of these aggregates in response to an increasing temperature causes an increase in the turbidity of the solution. This increase in turbidity correlates with a scattering of light, which is used to characterize the phase transition behavior of these polypeptides. Figure 1A shows the turbidity of 10  $\mu$ M Bac-ELP1-p21 and Bac-ELP2-p21 polypeptide solutions as a function of temperature. Solutions of both polypeptides are clear below the physiological temperature, but as the temperature is increased above 41°C, there is a sharp increase in the turbidity of Bac-ELP1-p21 which is reflected by the steep transition curve. At this concentration in PBS, Bac-ELP1-p21 has a  $T_t$  of 43 °C. Alternatively, the  $T_t$  of Bac-ELP2-p21 is 69 °C. Thus, Bac-ELP2-p21 and ELP2 containing constructs serve as a useful control to differentiate the effect of hyperthermia from the effect of aggregated Bac-ELP1-p21 polypeptide. The transition of each polypeptide

was reversible (data not shown), which is consistent with previously reported thermal properties of ELPs.<sup>19</sup>

The  $T_t$  of ELP is also dependent on the ELP concentration, as well as the concentration of other co-solutes. Therefore, in order to determine what concentration range of ELP is useful for thermal targeting under cell culture conditions, we determined the  $T_t$  of a range of concentrations of Bac-ELP1-p21 in cell culture media containing 10% FBS. As shown in Figure 1B, the  $T_t$  is inversely related to the polypeptide concentration. When  $T_t$  is plotted versus polypeptide concentration, the resulting curve can be fit with a logarithmic equation. Using this fitting method and extrapolation (Figure 1C), we determined that the useful window for Bac-ELP1-p21 thermal targeting (the concentration range in which the  $T_t$  lies between 37 and 42 °C) is between 12  $\mu$ M and 52  $\mu$ M.

The  $T_t$  of the rhodamine labeled Bac-ELP1-p21 was also determined and was within 2 °C of the unlabeled protein, insuring that the rhodamine label does not interfere with the aggregation of the polypeptide (data not shown).

### Intracellular localization of Bac-ELP1-p21 by confocal microscopy

Confocal microscopy of rhodamine-labeled Bac-ELP-p21 was used to confirm that the Bac CPP was capable of delivering the polypeptide to the cell interior and to determine the polypeptide's subcellular localization. SKOV-3 cells were exposed to rhodamine labeled Bac-ELP1-p21 (20  $\mu$ M) for 1 h at 37°C or 42°C, and cells were stained with a tubulin antibody to mark the cytoplasm and imaged either immediately or 24 h after exposure to the polypeptides. Images taken immediately after the 1 h polypeptide exposure showed predominantly membrane and cytoplasmic staining (Figure 2A), and cells treated at 42 °C had large polypeptide aggregates on the membrane and in the cytoplasm. Images taken 24 h later showed both cytoplasmic and nuclear staining in heated and unheated cells (Figure 2B). This observation is consistent with the previous study<sup>33</sup>, in which Bac was shown to deliver ELP to the nucleus in a percentage of the cells, and the percentage of staining nuclei increased with polypeptide concentration and time after exposure. To confirm that the observed localization is not the product of a fixation artifact, confocal images of live cells were also collected 24 h after polypeptide treatment. As shown in Figure 2C, the localization in live cells agrees quite well with the observed localization in fixed cells.

### Effect of polypeptides on cell proliferation

In order to examine the effect of polypeptides on cell proliferation, SKOV-3 cells were treated with Bac-ELP1-p21 or Bac-ELP2-p21 for 1 h at 37°C or 42°C in a concentration dependent manner. As shown in Figure 3A, treatment of SKOV-3 cells with Bac-ELP1-p21 at 37°C did not have any effect at 10 and 20  $\mu$ M, and only a slight effect at 30  $\mu$ M. However, treatment of the cells with 20 and 30  $\mu$ M of the same polypeptide at 42°C resulted in nearly 50% and 60% inhibition of cell proliferation, respectively. Similarly, SKOV-3 cells treated for 1 h at 37 or 42 °C with different concentrations of polypeptides and analyzed after 6 days showed an even greater inhibition of proliferation in heated samples as compared to unheated samples (Figure 3B). We used the same 6 day assay to determine the effects of control polypeptides (20  $\mu$ M) lacking either the Bac CPP, the p21 peptide, or the ELP polypeptide, and the Bac-ELP2-p21 non-thermally responsive control. As shown in Figure 3C, there was no effect on the cell proliferation on treatment with control polypeptides Bac-ELP1 (without the p21 inhibitory peptide), ELP1-p21 (without the Bac CPP), Bac-ELP2-p21 (does not aggregate in response to hyperthermia at 42°C) or p21 peptide at 37°C or 42°C. Hyperthermia itself also did not have any effect on the cell proliferation as untreated cells at 37°C or 42°C showed no difference in cell survival. In order to support the MTS proliferation assay, the proliferation rate of SKOV-3 cells was

measured using daily cell counts following treatment with Bac-ELP1-p21 or Bac-ELP1 control at 20  $\mu$ M for 1 h at 37 °C or 42 °C. Untreated and Bac-ELP1 treated cells showed approximately 3 doublings during the 6 day experiment. Bac-ELP1-p21 treated cells at 37°C showed a proliferation pattern similar to control and untreated cells, whereas Bac-ELP1-p21 treated cells combined with hyperthermia showed less than one doubling at the end of day 6 (Figure 3D). These results suggest that the inhibition of cell proliferation by Bac-ELP1-p21 in combination with hyperthermia is primarily due to its phase transition and not hyperthermia itself.

### Effect of Bac-ELP1-p21 on cell cycle distribution

Previous studies have shown that p21 inhibits the growth of cells by interacting mainly with cyclinD/ E-CDK2/ 4 and negatively modulates cell cycle progression.<sup>41</sup> Therefore, we examined the effect of 20  $\mu$ M Bac-ELP1-p21 treatment on the cell cycle in heated and non-heated cells. As shown in Figure 4, there was an increase in S-phase and G2/M-phase cells at the expense of G1 phase cells in heated cells harvested 24 h (Figure 4A) and 48 h (Figure 4B) after treatment, whereas no difference was observed in the distribution of the cell cycle phases in non-heated cells. Also, no effect was seen with the control polypeptide Bac-ELP1, which suggests that the ability to arrest the cell cycle is due to the p21 peptide moiety of the thermally delivered Bac-ELP1-p21 polypeptide.

In order to confirm these results and obtain a more accurate estimation of the fraction of cells in S phase, the experiment was repeated using BrdU incorporation to mark the cells in S phase during a short BrdU pulse. As shown in Figure 4C, this assay confirms the results obtained by simple PI staining. Hyperthermia alone had no effect on the cell cycle, and the distribution determined by the BrdU incorporation assay agreed with the PI assay. Bac-ELP1-p21 treatment at 42 °C caused an increase in the number of cells in S phase and in G2/ M, which was also in agreement with the PI results. The 37 °C treatments (not shown) also agreed with the results of the PI assay.

### Western blot analysis of Rb and pRb proteins

One of the important events in the cell cycle progression is hyperphosphorylation of the retinoblastoma protein.<sup>42</sup> The p21 peptide has been shown to prevent the cyclin/CDK-induced hyperphosphorylation of the retinoblastoma protein Rb.<sup>15</sup> Therefore, we measured the effect of polypeptide treatment on the hypo-phosphorylated (Rb) and hyper-phosphorylated (pRb) levels at 42°C. As shown in Figure 5, 24 h after treatment with Bac-ELP1-p21 for 1 h at 42°C, cells showed a significant decrease in the pRb levels as compared to untreated or Bac-ELP1 treated cells. The total Rb level was unchanged, and  $\beta$ -tubulin blotting was used to confirm accurate gel loading. These results suggest that Bac-ELP1-p21 most likely blocks the cell cycle by inhibiting the phosphorylation of the Rb protein.

### Induction of caspase activation by Bac-ELP1-p21

Caspases play an important role in the apoptosis mediated cell death and have been shown to be activated following cell cycle arrest by p21<sup>Waf1/Cip1</sup>.<sup>43</sup> In order to determine if caspase-mediated apoptosis is responsible for cell death following cell cycle arrest by the Bac-ELP1-p21 inhibitory polypeptide, cells were treated for 1 h at 37 or 42°C with the indicated polypeptides. Cells were harvested at various time intervals to check for poly-caspase activity by incubation with a fluorescent-caspase inhibitor and flow cytometry analysis. A histogram of fluorescence intensity versus cell number showed two peaks. Cells under the high intensity peak were quantified as cells with active caspases, whereas cells with low intensity represented caspase inactive cells. There was no effect of hyperthermia treatment alone on caspase activity. Also, treatment with the control polypeptide lacking the p21 peptide at both temperatures showed no caspase activity. As shown in Figure 6A, there was



a significant increase in the number of caspase positive cells on treatment with Bac-ELP1-p21 at 42°C. In addition, the percentage of cells with active caspases increased with time up to 72 h after Bac-ELP1-p21 and hyperthermia treatment. Only a slight increase in caspase positive cells was observed in non-heated cells treated with Bac-ELP1-p21.

In order to confirm that Bac-ELP1-p21 was inducing caspase activity, we examined Bac-ELP1-p21 treated cells for cleavage of poly (ADP-ribose) polymerase (PARP), which is cleaved by caspase 3 from a 116 kDa form to an 85 kDa form. SKOV-3 cells were treated with 20 μM Bac-ELP1 or Bac-ELP1-p21 for 1 h at 37 or 42 °C. 24 h after treatment, cells were harvested, and PARP cleavage was detected by Western blotting. As shown in Figure 6B, there was minimal PARP cleavage in untreated or Bac-ELP1 treated cells at either treatment temperature. In contrast, about 50% of the cellular PARP was found in the cleaved form 24 h after 37 °C exposure to Bac-ELP1-p21, and, 24 h after 42 °C exposure, nearly all the PARP existed in the cleaved 85 kDa form. These results support the flow cytometry assay and indicate that caspase-mediated apoptosis is a downstream effect of treatment with the Bac-ELP1-p21 polypeptide.

### Ability of Bac-ELP-p21 to inhibit the proliferation of other cell types

This study was carried out using SKOV-3 cells because their lack of p53 expression makes them an ideal model for human cancers in which p53 expression is lost. However, we also wished to determine the ability of Bac-ELP1-p21 to inhibit the proliferation of other cell types with varying p53 status. We repeated the 3 day cell proliferation assay described above with MCF-7 breast cancer cells (wild type p53) and Panc-1 pancreatic cancer cells (mutant (R273H) p53). As shown in Figure 7, 37 °C treatment with Bac-ELP1-p21 had little effect on either cell line. However, when Bac-ELP1-p21 treatment was combined with hyperthermia, proliferation of both cell lines was greatly inhibited. Furthermore, the potency of Bac-ELP1-p21 is similar in both MCF-7 and Panc-1, and slightly more potent in these cell lines than in SKOV-3. These results confirm that the p21 peptide acts downstream of p53, and inhibition by this peptide is not dependent on the cell's p53 status.

### Discussion

Previous *in vivo* studies have suggested that ELPs have potential as macromolecular carriers for a variety of therapeutic molecules or peptides that can be conjugated to these polypeptides.<sup>36, 37</sup> We have previously taken advantage of the fact that the ELP polymer is genetically encoded and have introduced a therapeutic peptide which inhibits c-Myc transcriptional function and proliferation of MCF-7 breast cancer cells.<sup>37</sup> We have also shown that CPP mediated intracellular delivery of ELP fused to the p21 peptide was capable of inhibiting cancer cell proliferation.<sup>29</sup> The present study extends the pilot work with the p21 peptide by adding the Bac CPP, and demonstrating the ability of Bac-ELP-p21 to target the nucleus and inhibit proliferation by arresting the cell cycle and inducing apoptosis in a temperature dependent manner.

We report here that Bac-ELP1-p21 treatment at 37°C had no effect on human ovarian cancer SKOV-3 cell proliferation. However, application of hyperthermia caused a concentration dependent decrease in the cell proliferation (Figure 3A & 3B). When hyperthermia is applied with thermally unresponsive ELP2 based constructs ( $T_1 > 60$  °C), there was no effect on cell proliferation. This suggests that the inhibitory effect of Bac-ELP1-p21 is greatly enhanced by the phase transition of ELP1. This is consistent with previous studies where thermally responsive ELP has been used to deliver different therapeutics like a c-Myc transcriptional inhibitory peptide (H1-S6A,F8A) <sup>37, 44</sup> and doxorubicin <sup>31, 45</sup>. The authors were able to show an enhanced antiproliferative effect of Pen-ELP-H1 and Tat-ELP1-GFLG-Dox when treatment with each polypeptide was combined with hyperthermia in

different cell lines.<sup>31, 37, 44</sup> Similar to the findings of the current study, the inhibition of cell proliferation observed in the previous studies was enhanced greatly by the hyperthermia induced phase transition of the ELP1 moiety, and not due to hyperthermia itself. The reason for this enhancement is that hyperthermia treatment induced ELP aggregation in the cell culture media. These aggregates bind to the cell surface, and are eventually internalized by endocytosis. Once the hyperthermia is removed, the polypeptides are free to re-dissolve and diffuse to their intracellular site of action. Therefore, the role of the hyperthermia treatment is simply to increase the amount of the polypeptide that is delivered into the cell <sup>31, 33, 37</sup>.

One of the limitations of therapeutic macromolecular carriers is their poor penetration capability through cellular plasma membranes. To overcome this limitation we fused ELP to the short cell penetrating peptide Bac. Cell penetrating peptides have been shown to deliver various cargos across the cell membrane.<sup>27, 28</sup> In our previous study, we were able to fuse various CPPs to ELP and enhance the uptake of ELP inside the cells.<sup>29, 30</sup> Since the molecular site of action of p21 is in the nucleus, in order to achieve its inhibitory effect on cell proliferation it is necessary to deliver the p21 mimicking peptide to the nuclear compartment. In a previous study, we showed that the Bac CPP can deliver the ELP polypeptide to the nucleus in a significant percentage of the cell population.<sup>33</sup> Here, we show that Bac can be used as a transduction domain to efficiently translocate the ELP macromolecular carrier fused to the p21 mimetic peptide across the plasma membrane and into the nuclear compartment. The polypeptide ELP1-p21 lacking the Bac transduction domain did not show any cytotoxicity at either the control or hyperthermia temperatures (Figure 3C).

In previous studies, it has been shown that various p21 peptide fragments arrest cells in the G1 and G2 stages, resulting in an inhibition of cell proliferation.<sup>15, 46, 47</sup> In this work, we have shown that Bac-ELP1-p21 arrests cells predominantly in the S-phase and the G2/M-phase (Figure 4). This cell cycle arrest may be due to the interaction of p21 with various cell cycle regulators, like cyclins and CDKs, that inhibits their complex formation.<sup>34</sup> One of the regulators of the cell cycle progression is the Retinoblastoma (Rb) protein.<sup>42</sup> In rapidly proliferating cells, Rb is usually in the hyperphosphorylated form (pRb), thereby leaving the transcription factor E2F free to activate transcription. Hypophosphorylated Rb binds E2F, prevents transcription activation, and causes cell cycle arrest. Our results indicated that there was a decrease in the pRb levels after treatment with Bac-ELP1-p21 in heated cells, without any significant change in Rb levels (Figure 5). Similarly, Ball et al. reported a decrease in hyperphosphorylated Rb protein on treatment with the p21 (141–160) peptide fused to the Antp cell penetrating peptide in human-keratinocyte-derived HaCaT cells.<sup>15</sup> These results suggest that the mechanism of cell cycle arrest by Bac-ELP1-p21 is most likely mediated by inhibition of Rb phosphorylation.

In an attempt to determine the biological effect Bac-ELP1-p21, we investigated its role in mediating apoptosis. The role of p21 in apoptosis is controversial. While some studies suggest that it prevents apoptosis, other studies demonstrate that it actually plays a role in apoptosis.<sup>48</sup> Caspases play an important role in mediating apoptosis. Therefore, in this study, we investigated the effect of Bac-ELP1-p21 on caspase activity because p21<sup>Waf1/Cip1</sup> has been reported to be involved in the activation of caspases.<sup>43</sup> As shown in Figure 6, an increase in poly-caspase activity was observed in heated cells which had been treated with Bac-ELP1-p21 for 1 h, and these results were confirmed with a PARP cleavage assay. These results suggest that the observed inhibition of cell proliferation by Bac-ELP1-p21 may be a result of apoptotic cell death through the activation of caspases. This observation is consistent with the study of Baker et al., who reported that the C-terminus p21 conjugated to a Tat peptide was able to enter the nucleus of U251 cells and cause apoptosis, as visualized by TUNEL staining. The authors were able to show the co-localization of Tat-p21 with

PCNA and therefore suggested that interaction of p21 with PCNA interferes with PCNA's function, leading to apoptosis.<sup>49</sup>

This study provides further evidence that ELP is an effective vector for targeted delivery of therapeutics. As shown here, the role of ELP is not limited to the delivery of oncogenic inhibitory peptides and conventional chemotherapeutic drugs, but it may also be used for the delivery of cell cycle inhibitory peptides. In order to show that Bac-ELP1-p21 mediated cytotoxicity is not dependent on the p53 status of the cell line, we expanded our cell line screen beyond the p53 null cell line SKOV-3. It was observed that Bac-ELP1-p21 treatment for 1 h at 42°C resulted in a significant inhibition of proliferation in a MCF-7 breast carcinoma cell line (p53 wild type) and a p53 mutated Panc-1 cell line.

In the present study, we have shown that Bac-ELP1-p21 is a promising thermally responsive macromolecular carrier which has the potential to be thermally targeted to the tumor site. Since no effect was seen at normal physiological temperature with Bac-ELP1-p21, it is very unlikely that it will cause any adverse effects in non heated tissues. Another advantage associated with macromolecular ELP is that it can overcome multidrug resistance.<sup>31</sup> Its use as a vector for the delivery of therapeutic drugs and peptides is attractive because, apart from the passive targeting due to the macromolecular nature of ELP, it can be actively targeted to the tumor site by application of heat. By attaching different CPPs to ELP it can also be targeted specifically to either the cytoplasmic compartment or to the nucleus. Because it is genetically encoded, ELP may be easily applied as a targeted macromolecular carrier for other inhibitors. Further *in vivo* studies of tumor reduction efficacy and polypeptide-induced toxicity and immunogenicity are necessary to advance this technology toward clinical evaluation, and these studies are currently underway.

In conclusion, the results presented here demonstrate that genetically engineered ELP, which was modified with the Bac CPP and a p21 mimetic peptide, inhibited the proliferation of SKOV-3 cells in combination with hyperthermia. This Bac-ELP1-p21 polypeptide has a transition temperature in the range of 39–42°C, making it a very good candidate for thermal targeting. We found that Bac-ELP1-p21 treatment at 42°C caused inhibition of Rb phosphorylation, arrest of the cell cycle, and activation of caspases. Such thermally responsive macromolecular biopolymers with antiproliferative activity would have great potential in cancer therapy for the thermally targeted treatment of solid tumors.

## Abbreviations

<b>CPP</b>	cell penetrating peptide
<b>Bac</b>	CPP from bactenecin
<b>EPR</b>	enhanced permeability and retention
<b>Tat</b>	CPP from HIV-1 transcription factor
<b>ELP</b>	Elastin-like polypeptide
<b>PBS</b>	phosphate buffered saline
<b>Rb</b>	retinoblastoma protein
<b>T<sub>t</sub></b>	transition temperature

## Acknowledgments

We wish to thank Ms. Rowshan Begum and Ms. Leslie Robinson for technical assistance and critical reading of the manuscript.

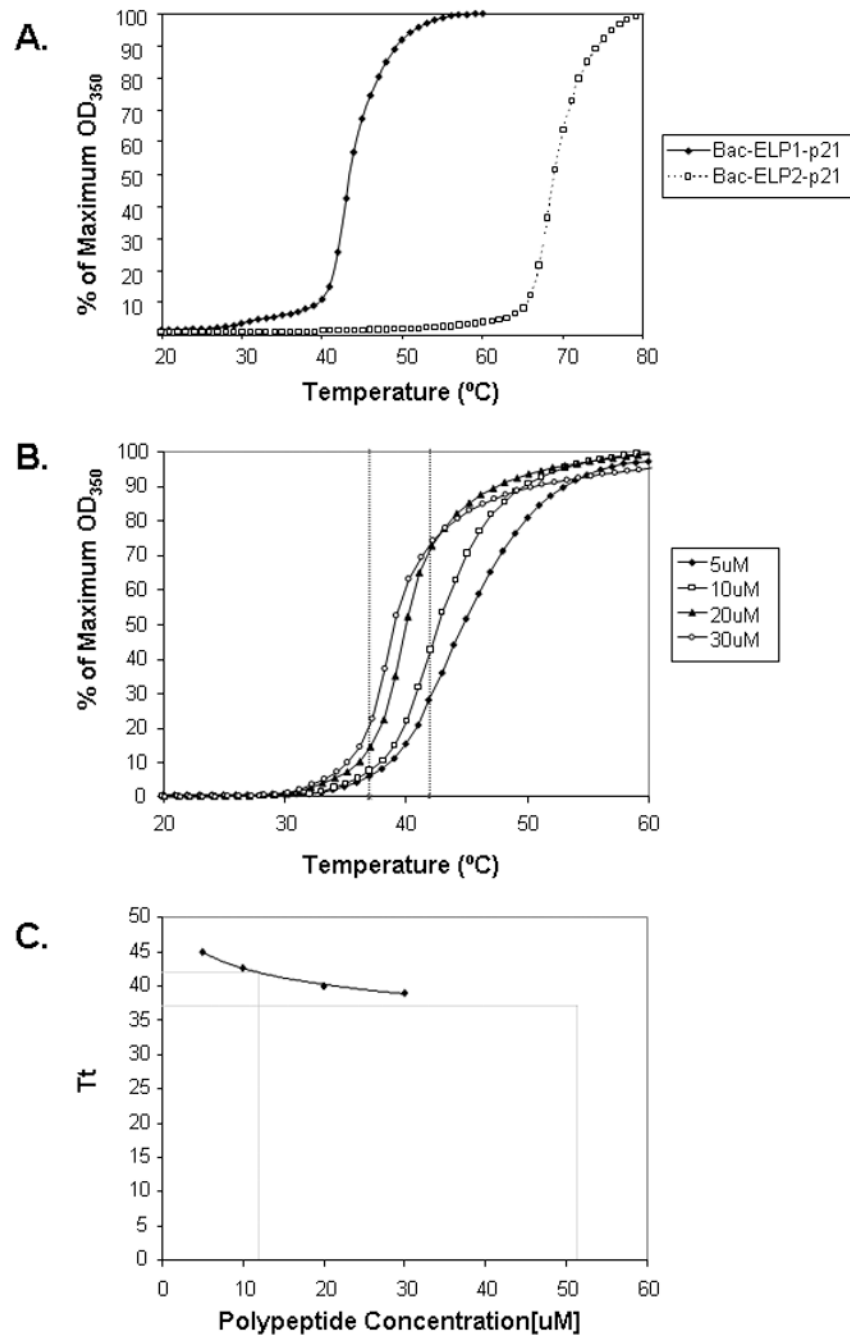
Grant sponsor: This study was supported by the National Institute of Health R21 CA113813-01A2 and Wendy Will Case Foundation grant.

## References

1. Allen TM. Liposomal drug formulation: rationale for development and what we can expect in the future. *Drugs*. 1998; 56:747–756. [PubMed: 9829150]
2. El-Aneed A. An overview of current delivery systems in cancer gene therapy. *J Control Release*. 2004; 94:1–14. [PubMed: 14684267]
3. Torchilin VP. Polymer-coated long-circulating microparticulate pharmaceuticals. *J.Microencapsul*. 1998; 15:1–19. [PubMed: 9463803]
4. Langer R. Drug delivery and targeting. *Nature (Lond.)*. 1998; 392 Suppl:5–10. [PubMed: 9579855]
5. Duncan R, Vicent MJ, Greco F, Nicholson RI. Polymer-drug conjugates: towards a novel approach for the treatment of endocrine-related cancer. *Endocr Relat Cancer*. 2005; 12 Suppl 1:S189–S199. [PubMed: 16113096]
6. Kopecek J, Kopeckova P, Minko T, Lu Z. HPMA copolymer-anticancer drug conjugates: design, activity, and mechanism of action. *Eur J Pharm Biopharm*. 2000; 50:61–81. [PubMed: 10840193]
7. Peer D, Karp JM, Hong S, Farokhzad OC, Margalit R, Langer R. Nanocarriers as an emerging platform for cancer therapy. *Nat Nanotechnol*. 2007; 2:751–760. [PubMed: 18654426]
8. Duncan R. Polymer conjugates as anticancer nanomedicines. *Nat Rev Cancer*. 2006; 6:688–701. [PubMed: 16900224]
9. Takakura Y, Fujita T, Hashida M, Sezaki H. Disposition characteristics of macromolecules in tumor-bearing mice. *Pharm. Res*. 1990; 7:339–346. [PubMed: 1694582]
10. Maeda H, Seymour LW, Miyamoto Y. Conjugates of anticancer agents and polymers: advantages of macromolecular therapeutics in vivo. *Bioconjug.Chem*. 1992; 3:351–362. [PubMed: 1420435]
11. Cassidy J, Duncan R, Morrison GJ, Strohalm J, Plocova D, Kopecek J, Kaye SB. Activity of N-(2-hydroxypropyl)methacrylamide copolymers containing daunomycin against a rat tumour model. *Biochem. Pharmacol*. 1989; 38:875–879. [PubMed: 2930589]
12. Yamaoka T, Tabata Y, Ikada Y. Distribution and tissue uptake of poly(ethylene glycol) with different molecular weights after intravenous administration to mice. *J. Pharm.Sci*. 1994; 83:601–606. [PubMed: 8046623]
13. Gius DR, Ezhevsky SA, Becker-Hapak M, Nagahara H, Wei MC, Dowdy SF. Transduced p16INK4a peptides inhibit hypophosphorylation of the retinoblastoma protein and cell cycle progression prior to activation of Cdk2 complexes in late G1. *Cancer Res*. 1999; 59:2577–2580. [PubMed: 10363976]
14. Hosotani R, Miyamoto Y, Fujimoto K, Doi R, Otaka A, Fujii N, Imamura M. Trojan p16 peptide suppresses pancreatic cancer growth and prolongs survival in mice. *Clin Cancer Res*. 2002; 8:1271–1276. [PubMed: 11948142]
15. Ball KL, Lain S, Fahraeus R, Smythe C, Lane DP. Cell-cycle arrest and inhibition of Cdk4 activity by small peptides based on the carboxy-terminal domain of p21WAF1. *Curr Biol*. 1997; 7:71–80. [PubMed: 8999999]
16. Bonfanti M, Taverna S, Salmona M, D'Incalci M, Broggin M. p21WAF1-derived peptides linked to an internalization peptide inhibit human cancer cell growth. *Cancer Res*. 1997; 57:1442–1446. [PubMed: 9108443]
17. Urry DW, Luan C-H, Parker TM, Gowda DC, Prasad KU, Reid MC, Safavy A. Temperature of Polypeptide Inverse Temperature Transition Depends on Mean Residue Hydrophobicity. *J. Am. Chem. Soc*. 1991; 113:4346–4348.
18. Tatham AS, Shewry PR. Elastomeric proteins: biological roles, structures and mechanisms. *Trends Biochem Sci*. 2000; 25:567–571. [PubMed: 11084370]
19. Meyer DE, Kong GA, Dewhirst MW, Zalutsky MR, Chilkoti A. Targeting a Genetically Engineered Elastin-like Polypeptide to Solid Tumors by Local Hyperthermia. *Cancer Res*. 2001; 61:1548–1554. [PubMed: 11245464]

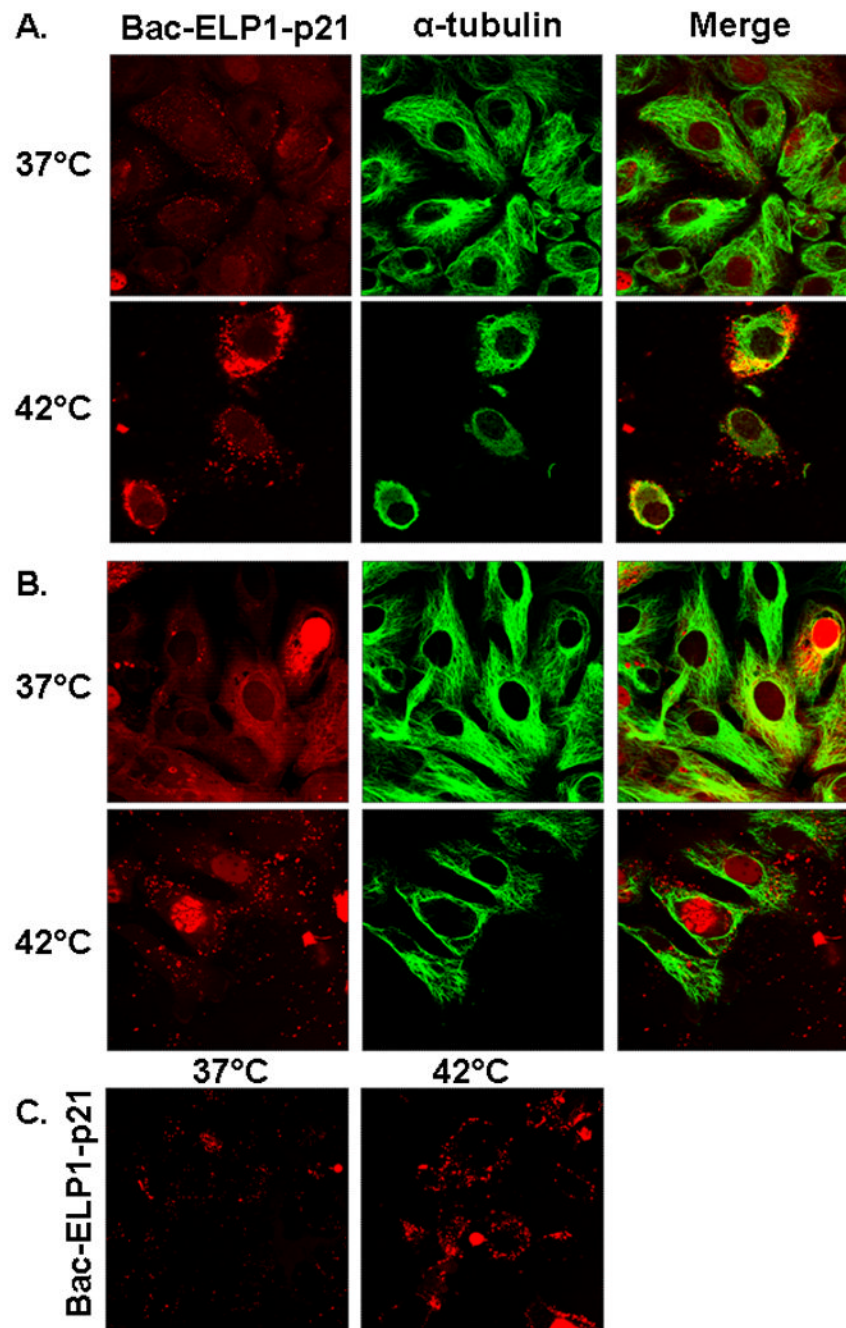
20. Liu W, Dreher MR, Furgeson DY, Peixoto KV, Yuan H, Zalutsky MR, Chilkoti A. Tumor accumulation, degradation and pharmacokinetics of elastin-like polypeptides in nude mice. *J Control Release*. 2006; 116:170–178. [PubMed: 16919353]
21. Dreher MR, Liu W, Michelich CR, Dewhirst MW, Chilkoti A. Thermal cycling enhances the accumulation of a temperature-sensitive biopolymer in solid tumors. *Cancer Res*. 2007; 67:4418–4424. [PubMed: 17483356]
22. Fujiwara K, Watanabe T. Effects of hyperthermia, radiotherapy and thermoradiotherapy on tumor microvascular permeability. *Acta Pathol Jpn*. 1990; 40:79–84. [PubMed: 2160185]
23. Gerlowski LE, Jain RK. Effect of hyperthermia on microvascular permeability to macromolecules in normal and tumor tissues. *Int J Microcirc Clin Exp*. 1985; 4:363–372. [PubMed: 4086191]
24. Jain RK. Transport of molecules across tumor vasculature. *Cancer Metastasis Rev*. 1987; 6:559–593. [PubMed: 3327633]
25. Temsamani J, Guinot P. Antisense oligonucleotides: a new therapeutic approach. *Biotechnology & Applied Biochemistry*. 1997; 26:65–71. [PubMed: 9357101]
26. Snyder EL, Meade BR, Saenz CC, Dowdy SF. Treatment of terminal peritoneal carcinomatosis by a transducible p53-activating peptide. *PLoS Biol*. 2004; 2:E36. [PubMed: 14966535]
27. Nori A, Kopecek J. Intracellular targeting of polymer-bound drugs for cancer chemotherapy. *Adv Drug Deliv Rev*. 2005; 57:609–636. [PubMed: 15722167]
28. Temsamani J, Vidal P. The use of cell-penetrating peptides for drug delivery. *Drug Discov Today*. 2004; 9:1012–1019. [PubMed: 15574317]
29. Massodi I, Bidwell GL 3rd, Raucher D. Evaluation of cell penetrating peptides fused to elastin-like polypeptide for drug delivery. *J Control Release*. 2005; 108:396–408. [PubMed: 16157413]
30. Massodi I, Raucher D. A thermally responsive Tat-elastin-like polypeptide fusion protein induces membrane leakage, apoptosis, and cell death in human breast cancer cells. *J Drug Target*. 2007; 15:611–622. [PubMed: 17968715]
31. Bidwell GL 3rd, Fokt I, Priebe W, Raucher D. Development of elastin-like polypeptide for thermally targeted delivery of doxorubicin. *Biochem Pharmacol*. 2007; 73:620–631. [PubMed: 17161827]
32. Sadler K, Eom KD, Yang JL, Dimitrova Y, Tam JP. Translocating proline-rich peptides from the antimicrobial peptide bactenecin 7. *Biochemistry*. 2002; 41:14150–14157. [PubMed: 12450378]
33. Bidwell GL 3rd, Davis AN, Raucher D. Targeting a c-Myc inhibitory polypeptide to specific intracellular compartments using cell penetrating peptides. *J Control Release*. 2009; 135:2–10. [PubMed: 19095020]
34. Mutoh M, Lung FD, Long YQ, Roller PP, Sikorski RS, O'Connor PM. A p21(Waf1/Cip1)carboxyl-terminal peptide exhibited cyclin-dependent kinase-inhibitory activity and cytotoxicity when introduced into human cells. *Cancer Res*. 1999; 59:3480–3488. [PubMed: 10416614]
35. Warbrick E, Lane DP, Glover DM, Cox LS. A small peptide inhibitor of DNA replication defines the site of interaction between the cyclin-dependent kinase inhibitor p21WAF1 and proliferating cell nuclear antigen. *Curr Biol*. 1995; 5:275–282. [PubMed: 7780738]
36. Chilkoti A, Dreher MR, Meyer DE. Design of thermally responsive, recombinant polypeptide carriers for targeted drug delivery. *Adv Drug Deliv Rev*. 2002; 54:1093–1111. [PubMed: 12384309]
37. Bidwell GL 3rd, Raucher D. Application of thermally responsive polypeptides directed against c-Myc transcriptional function for cancer therapy. *Mol Cancer Ther*. 2005; 4:1076–1085. [PubMed: 16020665]
38. Meyer DE, Chilkoti A. Purification of Recombinant Proteins by Fusion with Thermally Responsive Polypeptides. *Nat.Biotechnol*. 1999; 17:1112–1115. [PubMed: 10545920]
39. Tomasinsig L, Skerlavaj B, Papo N, Giabbai B, Shai Y, Zanetti M. Mechanistic and functional studies of the interaction of a proline-rich antimicrobial peptide with mammalian cells. *J Biol Chem*. 2006; 281:383–391. [PubMed: 16257969]
40. Mattock H, Lane DP, Warbrick E. Inhibition of cell proliferation by the PCNA-binding region of p21 expressed as a GFP miniprotein. *Exp Cell Res*. 2001; 265:234–241. [PubMed: 11302688]

41. Brugarolas J, Moberg K, Boyd SD, Taya Y, Jacks T, Lees JA. Inhibition of cyclin-dependent kinase 2 by p21 is necessary for retinoblastoma protein-mediated G1 arrest after gamma-irradiation. *Proc Natl Acad Sci U S A*. 1999; 96:1002–1007. [PubMed: 9927683]
42. Giacinti C, Giordano A. RB and cell cycle progression. *Oncogene*. 2006; 25:5220–5227. [PubMed: 16936740]
43. Huo JX, Metz SA, Li GD. p53-independent induction of p21(waf1/cip1) contributes to the activation of caspases in GTP-depletion-induced apoptosis of insulin-secreting cells. *Cell Death Differ*. 2004; 11:99–109. [PubMed: 12970678]
44. Bidwell GL 3rd, Raucher D. Enhancing the antiproliferative effect of topoisomerase II inhibitors using a polypeptide inhibitor of c-Myc. *Biochem Pharmacol*. 2006; 71:248–256. [PubMed: 16316634]
45. Bidwell GL 3rd, Davis AN, Fokt I, Priebe W, Raucher D. A thermally targeted elastin-like polypeptide-doxorubicin conjugate overcomes drug resistance. *Invest New Drugs*. 2007; 25:313–326. [PubMed: 17483874]
46. Tunnemann G, Martin RM, Haupt S, Patsch C, Edenhofer F, Cardoso MC. Cargo-dependent mode of uptake and bioavailability of TAT-containing proteins and peptides in living cells. *Faseb J*. 2006; 20:1775–1784. [PubMed: 16940149]
47. Luo Y, Hurwitz J, Massague J. Cell-cycle inhibition by independent CDK and PCNA binding domains in p21Cip1. *Nature*. 1995; 375:159–161. [PubMed: 7753174]
48. Gartel AL, Tyner AL. The role of the cyclin-dependent kinase inhibitor p21 in apoptosis. *Mol Cancer Ther*. 2002; 1:639–649. [PubMed: 12479224]
49. Baker RD, Howl J, Nicholl ID. A synchological cell penetrating peptide mimic of p21(WAF1/CIP1) is pro-apoptogenic. *Peptides*. 2007; 28:731–740. [PubMed: 17287047]



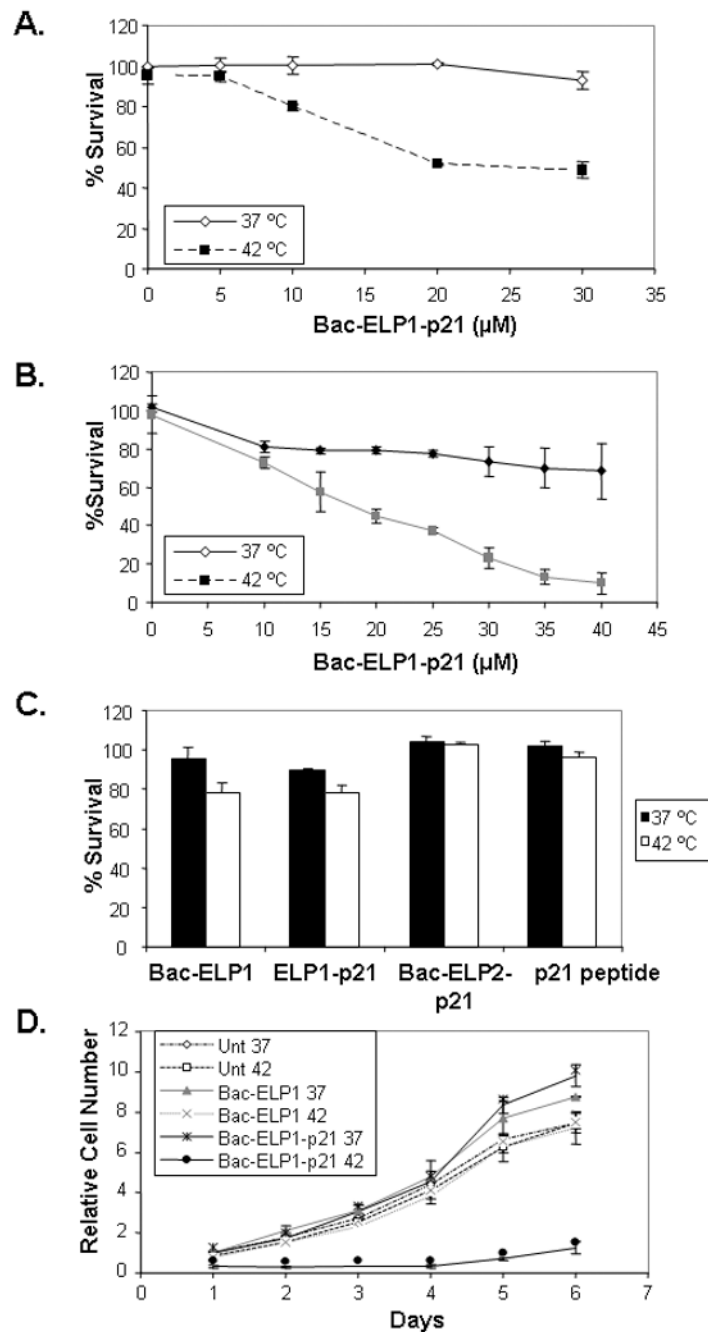
**FIGURE 1.**

Thermal properties of Bac-ELP-p21 polypeptide. **A.** The turbidity profiles of 10  $\mu\text{M}$  of Bac-ELP1-p21 and Bac-ELP2-p21 in PBS were obtained by heating at a rate of  $1^{\circ}\text{C}/\text{min}$ . The transition temperature  $T_t$  was defined from the heating profile as the temperature at which 50% turbidity of the polypeptide solution occurred. **B.** *The concentration dependence of the  $T_t$  was determined by monitoring the turbidity of a solution of various concentration of Bac-ELP1-p21 in cell culture media while heating.* **C.** *The data in (B) was used to determine the  $T_t$  at each polypeptide concentration, and a plot of  $T_t$  versus concentration was fit using a logarithmic equation to determine the effective concentration window for Bac-ELP1-p21 thermal targeting.*



**FIGURE 2.** Subcellular localization of *rhodamine labeled* Bac-ELP1-p21 in SKOV-3 cells as visualized by confocal microscopy. Cells were treated with 20  $\mu$ M of *rhodamine-labeled* Bac-ELP1-p21 at 37°C or 42°C for 1 h. Confocal images were taken (A) 1 h and (B) 24 h later. *Tubulin was stained as a reference for cellular structure. The subcellular distribution of Bac-ELP1-p21 was also confirmed in live cells 24 h after a 1 h exposure at 37 or 42 °C (C).* Fluorescence intensity in the heated samples was greater and the gain was adjusted for these samples before image acquisition. Therefore, these images are not quantitative.



**FIGURE 3.**

Effect of polypeptide treatment on SKOV-3 cell proliferation. Cell proliferation measured after treatment with different polypeptides for 1 h at the indicated concentration and temperature. **A.** Cell proliferation measured by MTS assay after 3 days. **B.** Cell proliferation measured by MTS assay after 6 days. **C.** Cell proliferation 6 days after treatment with 20 μM control polypeptides. Results are represented as mean ± SEM of 3–5 independent experiments. **D.** Proliferation rate of SKOV-3 cells was determined by daily cell counts following a 1 h exposure to the indicated polypeptide (20 μM) at 37 or 42 °C. Daily counts are expressed relative to the counts on day 1, and the data represents an average of 3–5 experiments. Bars- ± SEM.

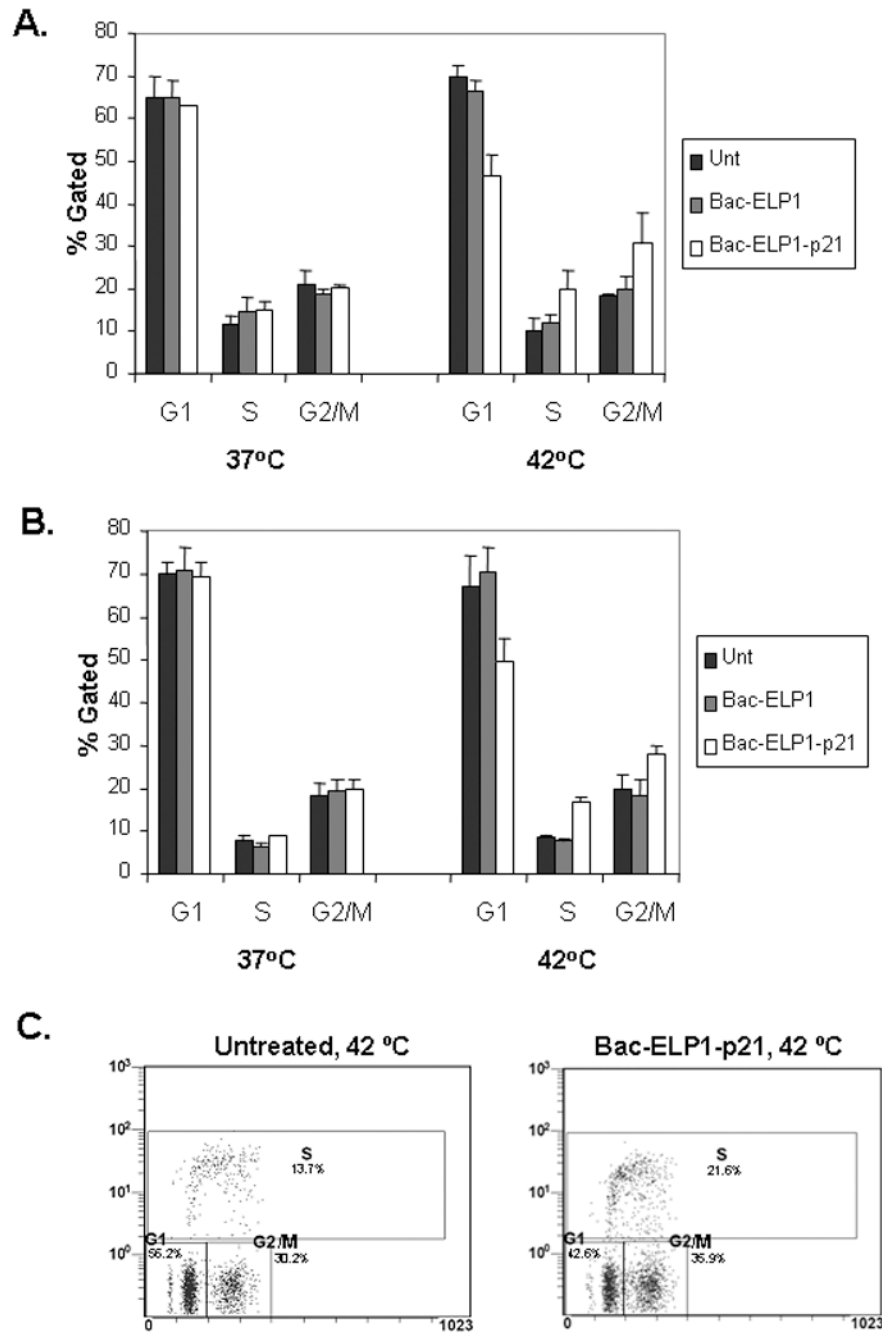


**FIGURE 4.** Effect of Bac-ELP-p21 on cell cycle progression of SKOV-3 cells. Cells were treated with 20  $\mu$ M of polypeptides at 37 or 42 °C for 1 h. Cells were harvested after 24 h (A) or 48 h (B), stained with PI, and analyzed by flow cytometry. Results are represented as mean  $\pm$  SEM of 3–5 independent experiments. C. SKOV-3 cells were treated as above and pulsed with BrdU (for 1 h) 24 h after treatment. Cells were immunostained with a FITC-labeled BrdU antibody, co-stained with PI, and analyzed by flow cytometry. A representative scatter plot of untreated or Bac-ELP1-p21 (20  $\mu$ M), 42 °C treated cells is shown. Results following 37 °C treatment were also in agreement with the PI only assay (data not shown).

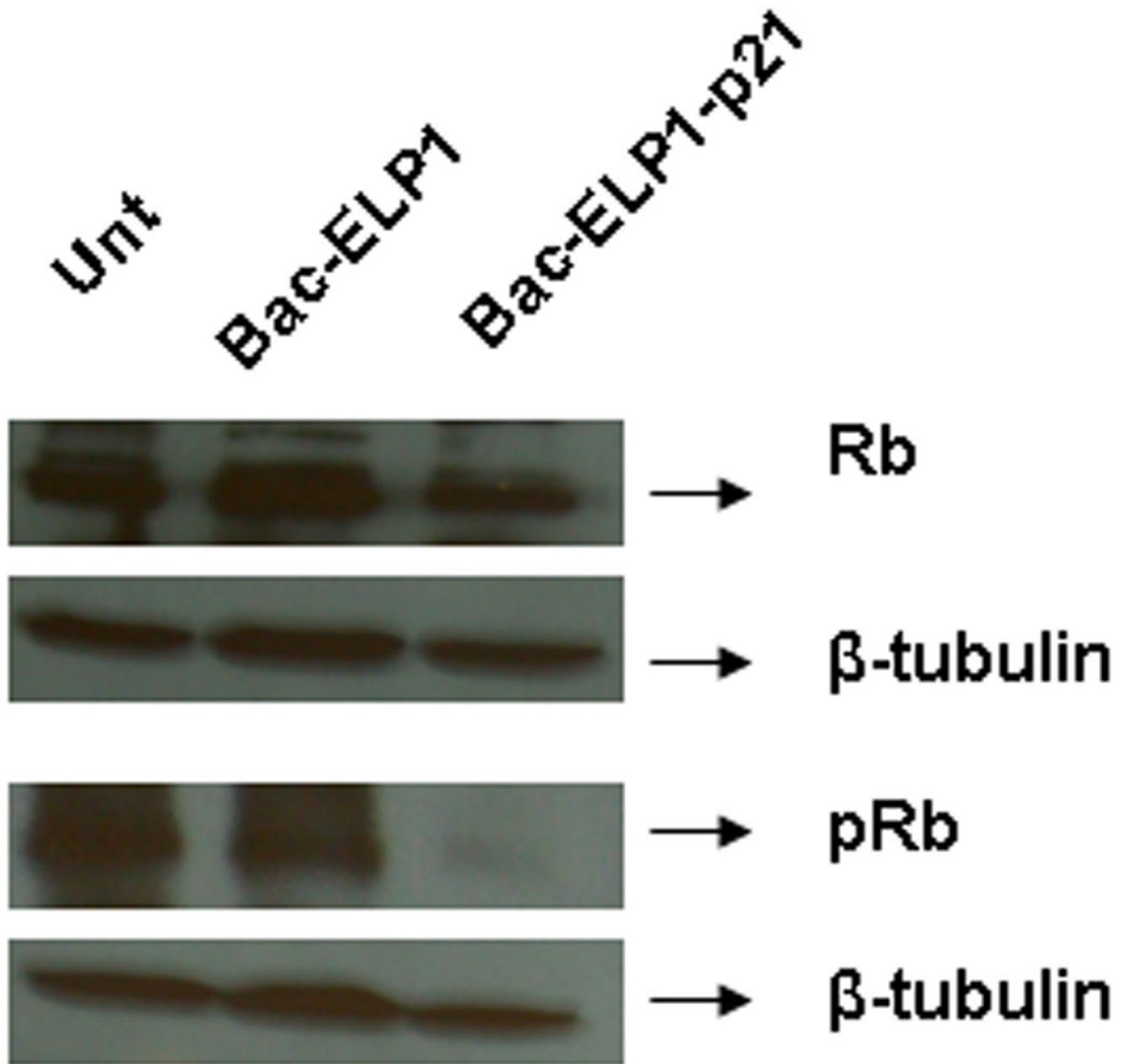


**FIGURE 5.** SDS-PAGE analysis of Rb protein in SKOV-3 cells following treatment with Bac-ELP1-p21. Cells were treated with the indicated polypeptide (30  $\mu$ M) at 42°C for 1 h, harvested 24 h later, and lysed. Equal amount of samples were loaded onto a 12% SDS gel, transferred to a blot which was probed with the indicated antibodies.

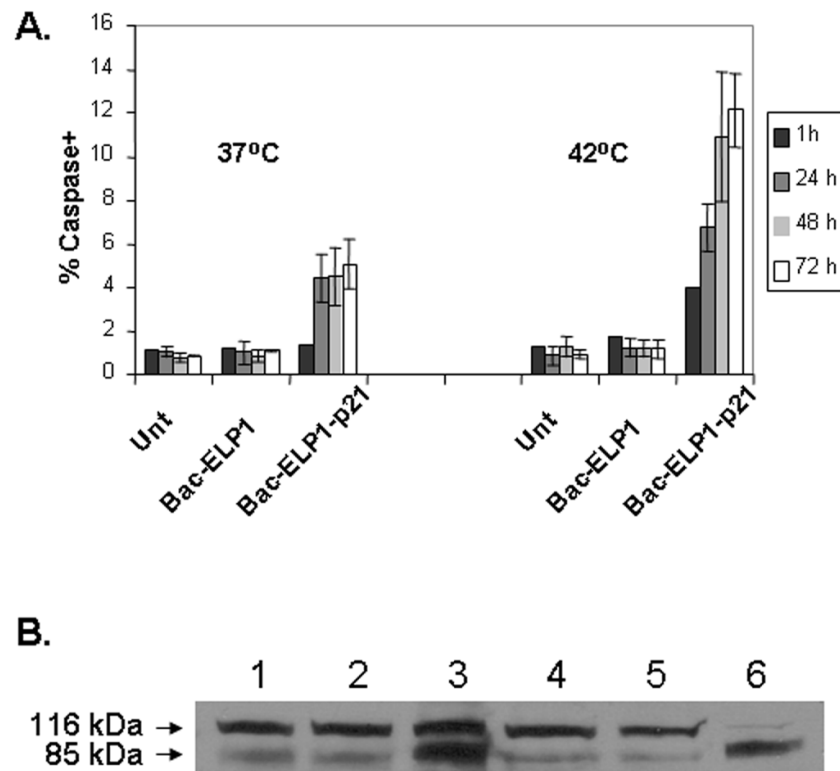


**FIGURE 6.** Effect of Bac-ELP-p21 on caspase activation of SKOV-3 cells. **A.** Cells were treated with 20  $\mu$ M of polypeptides at 37°C or 42°C for 1 h, harvested, washed with PBS and incubated with 10  $\mu$ l of 30 $\times$  FLICA reagent for 2 h and analyzed by flow cytometry. The data represents the average of  $\pm$  SEM of three independent experiments plotted as caspase positive cells normalized to untreated cells. **B.** Caspase activation was confirmed by assessing cleavage of PARP 24 h after polypeptide treatment (20  $\mu$ M) by Western blotting. Lane 1, untreated (37 °C); Lane 2, Bac-ELP1 (37 °C); Lane 3 (Bac-ELP1-p21 (37 °C); Lane 4, untreated (42 °C); Lane 5, Bac-ELP1 (42 °C); Lane 6 (Bac-ELP1-p21 (42 °C).

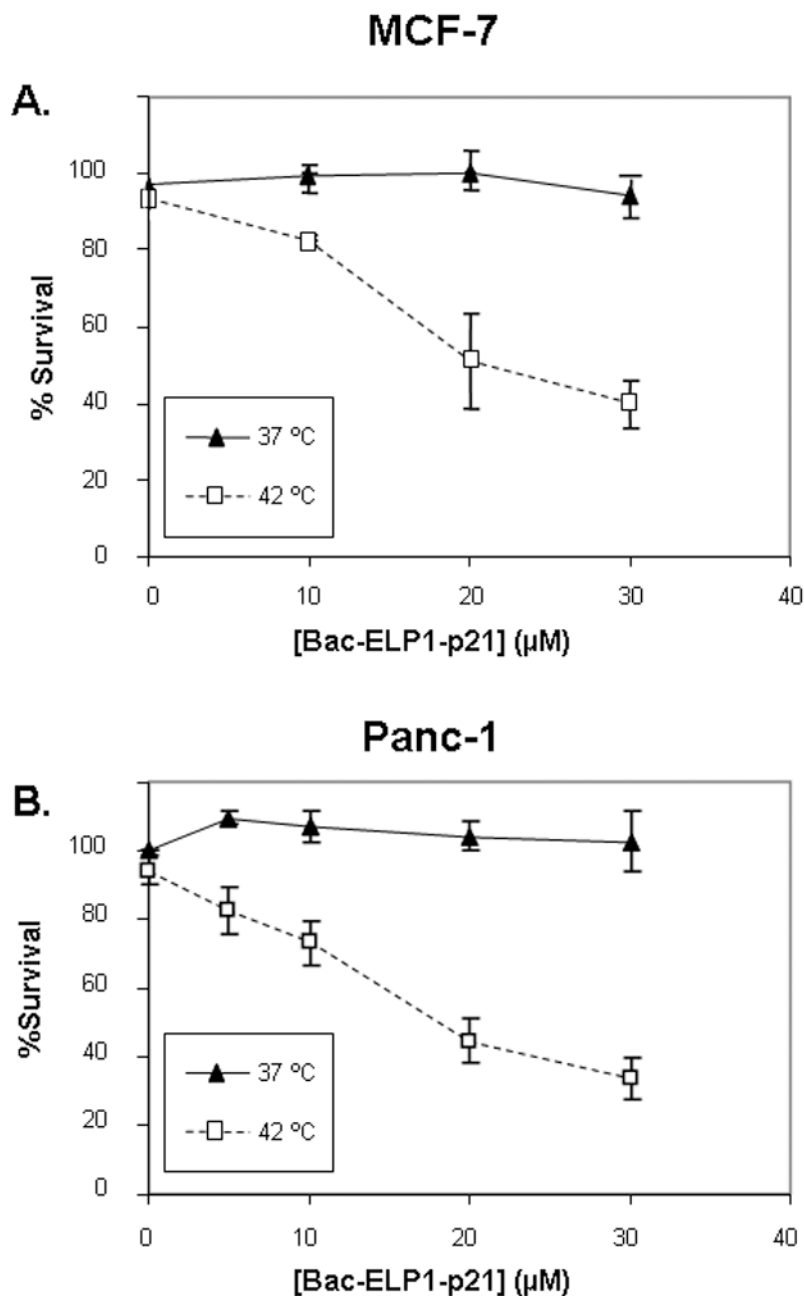


**FIGURE 7.** Inhibition of proliferation of other cell types by Bac-ELP1-p21. MCF-7 and Panc-1 cells were treated with the indicated concentration of Bac-ELP1-p21 at 37 or 42 °C, and cell proliferation was determined 3 days later using the MTS assay. Results shown are the mean  $\pm$  SEM of three independent experiments.